

# FRACTURE ANALYSIS OF THE FAA/NASA WIDE STIFFENED PANELS

B. R. Seshadri  
National Research Council Associate  
NASA Langley Research Center  
Hampton, Virginia, 23681-2199 USA  
Tel: 757-864-3478  
Fax: 757-864-8911  
b.r.seshadri@larc.nasa.gov

512-39  
037248

J. C. Newman, Jr., D. S. Dawicke and R. D. Young  
NASA Langley Research Center  
Hampton, Virginia, 23681-2199 USA

## ABSTRACT

This paper presents the fracture analyses conducted on the FAA/NASA stiffened and unstiffened panels using the STAGS (S<sup>TR</sup>uctural Analysis of General Shells) code with the critical crack-tip-opening angle (CTOA) fracture criterion. The STAGS code with the "plane-strain" core option was used in all analyses. Previous analyses of wide, flat panels have shown that the high-constraint conditions around a crack front, like plane strain, has to be modeled in order for the critical CTOA fracture criterion to predict wide panel failures from small laboratory tests. In the present study, the critical CTOA value was determined from a wide (unstiffened) panel with anti-buckling guides. The plane-strain core size was estimated from previous fracture analyses and was equal to about the sheet thickness. Rivet flexibility and stiffener failure was based on methods and criteria, like that currently used in industry. STAGS and the CTOA criterion were used to predict load-against-crack extension for the wide panels with a single crack and multiple-site damage cracking at many adjacent rivet holes. Analyses were able to predict stable crack growth and residual strength within a few percent (5%) of stiffened panel tests results but over predicted the buckling failure load on an unstiffened panel with a single crack by 10%.

## 1. INTRODUCTION

Widespread fatigue damage is of great concern to the aging commercial transport fleets because the residual strength of a stiffened structure with a single long crack may be significantly reduced by the existence of adjacent smaller cracks as postulated by Swift [1]. Whereas a single long crack in a fuselage structure may produce flapping, a process by which a cracked fuselage would peel open in a small local region and lead to safe decompression, a fuselage with a long lead crack and multiple-site or multiple-element damage (MSD or MED) cracking may not flap. Tests on panels with long lead cracks and MSD have shown that the presence of an array of small adjacent cracks strongly degrade residual strengths [2,3]. One of the objectives in the NASA Aging Aircraft Research Program [4] is to develop the methodology to predict flapping or failure in damaged fuselage structures in the presence of widespread fatigue damage. The approach is to use a finite-element shell code with global-local, adaptive mesh capabilities and appropriate local fracture criteria to predict progressive failure in complex structures. In the future, fuselage structures may be designed by analysis, and verified by tests, to produce flapping or improved crack arresting capability under MSD or MED conditions.

In an effort to develop the methodologies required to predict the residual strength of complex fuselage structures with MSD, a series of tests and analyses have been performed from the coupon level to

subscale fuselage simulation tests [5,6]. These series of tests were used to verify the residual strength methodology based on the critical crack-tip-opening angle (CTOA) failure criterion. NASA and the FAA have designed a series of wide, stiffened panels with single and multiple-site damage cracking at many simulated rivet holes [7,8]. These panels had "fatigue" MSD cracks instead of sawcuts. The panels were made of 2024-T3 sheet material (thickness of 1.6 mm) with five 7075-T6 stiffeners (thickness of 2.2 mm). Stiffeners were placed symmetrical about the thickness of the sheet. The central stiffeners were cut and the panels were allowed to buckle during the stable tearing and crack linkup process. Load-crack extension, load-strain records and out-of-plane displacement measurements were made during all tests.

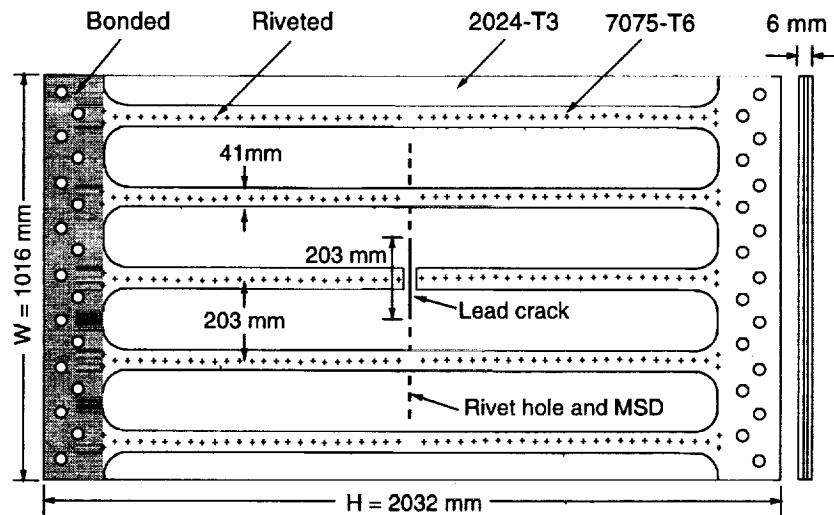
Stable crack growth in metallic materials has been studied extensively using elastic-plastic finite-element methods, see reference 9. These studies were performed to investigate various fracture criteria. Of these, the crack-tip-opening angle (CTOA) or displacement (CTOD) criterion was shown to be the most suited for modeling stable crack growth and instability during the fracture process. Numerous investigators have also experimentally measured CTOA (or CTOD) during fracture. Dawicke et al. [10], using a high-resolution photographic camera with a video system, has shown that the critical angles during stable crack growth in thin-sheet aluminum alloys were nearly constant after a small amount of tearing. The non-constant CTOA region (measured at the free surface) was shown to be associated with severe tunneling during the initiation of stable tearing. Newman and Dawicke [11] and Dawicke et al. [12] have extensively applied the CTOA fracture criterion and the finite-element method to analyze stable crack growth and fracture of many complex crack configurations made of aluminum alloys. Seshadri and Newman [13] have also used the finite-element method and the CTOA criterion to predict stable tearing in the presence of severe out-of-plane buckling for both aluminum alloys and steels.

This paper presents the fracture analyses conducted on the FAA/NASA stiffened panels using the STAGS (STructural Analysis of General Shells) code [14,15] with the critical crack-tip-opening angle (CTOA) fracture criterion. The STAGS code, with the "plane-strain" core option, was used in all analyses. Previous analyses of wide, flat panels have shown that the high-constraint conditions around a crack front, like plane strain, has to be modeled in order for the critical CTOA fracture criterion to predict wide panel failures from small laboratory tests [16]. In the present study, the critical CTOA value was determined from a wide (unstiffened) panel with anti-buckling guides. The plane-strain core size was estimated from previous fracture analyses and was about equal to the sheet thickness. Rivet flexibility and stringer failure were based on methods and criteria, like that currently used in industry [1]. Comparisons were made between load-crack extension on stiffened and unstiffened panels with single cracks and MSD. An assessment of the capability of the STAGS code with the critical CTOA failure criterion to predict residual strength was made.

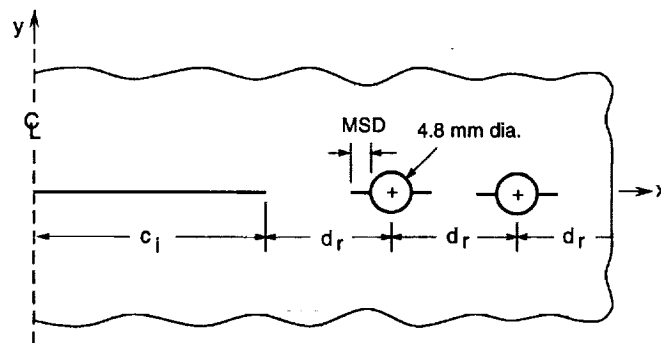
## 2. EXPERIMENTS

NASA Langley Research Center (LARC) and the FAA William J. Hughes Technical Center have jointly designed and sponsored fracture tests on 1016-mm wide sheets made of 1.6-mm thick 2024-T3 aluminum alloy with and without stiffeners [7,8]. Ten wide panel fracture tests were conducted at LARC. Half of the specimens had five 7075-T6 aluminum alloy stiffeners (41-mm wide, 2.2-mm thick) riveted on each side of the sheet with a spacing of 203 mm, as shown in Figure 1(a). The stiffeners were orientated in the direction of loading and perpendicular to the direction of the crack(s). The rivets were 2017-T4 aluminum alloy button head with a 25.4-mm rivet spacing ( $d_r$ ). The 7075/2024/7075 lay-up was bonded only in the grip area but riveted over the remainder of the sheet. The central stiffeners were cut along the crack line. Open holes were machined into the sheet at the required rivet spacing along the crack line but rivets were not installed. Holes were not machined into the stiffeners along the crack-line location. Five

different crack configurations were tested: a single center crack, a single center crack with an array of 12 holes (4.8-mm diameter) on either side of the lead crack, and a single center crack with three different equal multiple-site damage (MSD) cracking (0.25, 0.76 and 1.3-mm) at the edge of each hole. The MSD cracks were introduced into the test specimen by fatigue precracking at a low applied cyclic stress level [8]. Figure 1(b) shows the details of the crack configuration along the crack line. The lead crack half-length ( $c_i$ ) in all of the specimens was 101.5 mm. For each crack configuration, identical specimens were tested with and without riveted stringers. All tests were conducted under stroke control. During the tests, measurements were made of load, crack extension, applied end displacement, strain field in the crack-tip region, strains in the intact and broken stiffeners, and displacement fields (local and global).



(a) Stiffened panel



(b) Typical open-hole and MSD crack configuration

Figure 1. Stiffened panel and typical crack configuration analyzed

Test results on load-against-crack extension measured on the five stiffened panels [7,8] are shown in Figure 2. The first intact stringer was located at about 100 mm from the initial crack-tip location (see dashed line). Circular symbols show the results for the single crack. The large gap in the data was when the crack was underneath the stiffener. Once the crack emerged from under the stiffener, the panel failed (solid symbol). Square symbols show the results from the single crack with 12 open holes on each side of the crack. The vertical steps in the data (with no crack extension) was when the crack linked with an open hole, and additional load was required to fracture the material at edge of the hole. Again, the solid symbol denotes the maximum failure load on the panel. Results show that even a panel with a single

crack and only open holes fail at a significantly lower load than that of a specimen with a single crack. The three tests with different size MSD all behaved in a similar manner. After the lead crack linked with the MSD cracks and grew pass the stiffener, the sheet failed and all 24 MSD cracks linked. Panel failure then occurred at about a 10% higher load than sheet failure. These results show that MSD at open holes reduce the residual strength about 30% from that of a panel with only a single crack.

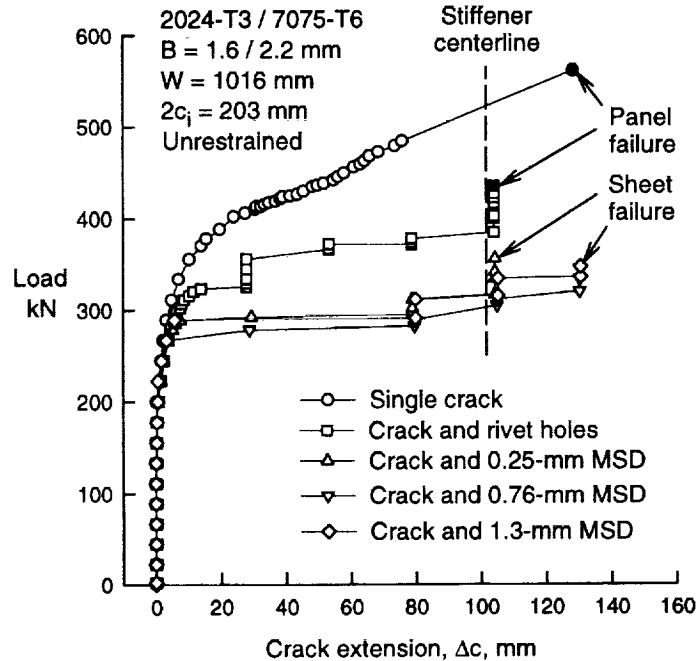


Figure 2. Load-against-crack extension from stiffened panel test program [7,8].

Large middle-crack tension panels (restrained against buckling) were tested to measure the critical crack-tip-opening angle (CTOA) on the 1.6-mm thick sheet 2024-T3 material during stable tearing and fracture. The critical CTOA is plotted against crack extension in Figure 3. The 610-mm wide specimen had an initial sawcut (254 mm in length) and the 1016-wide specimen had a large fatigue crack. During the fracture tests, a high-resolution camera and video system [10] was used to record the tearing crack. At each video image, corresponding to a given amount of crack extension, four to six measurements of the critical angle were measured from 0.5 to 1.5 mm from the crack tip. The average values are shown in Figure 3. The test measurements show an average angle of 5.15 degrees with a  $\pm 1$  degree of scatter. The critical CTOA was nearly constant over nearly two orders of magnitude in crack extension. For small amounts of crack extension (less than sheet thickness), larger CTOA values are generally measured on the surface of the specimen, possibly due to severe crack tunneling (see ref. 12).

### 3. ANALYSES

The STAGS finite-element shell code [14,15] and the critical crack-tip-opening angle (CTOA) failure criterion were used to model stable tearing of cracks and residual strength behavior of wide, flat-unstiffened and flat-stiffened panels made of 2024-T3 aluminum alloy sheet and 7075-T6 stiffeners. Rivet connectivity, rivet yielding, stiffener yielding, out-of-plane buckling and stiffener-sheet contact behavior were modeled during the stable tearing process. Single cracks and multiple-site-damage (MSD) cracks at simulated rivet holes were considered. The holes, used to produce the MSD cracks, were only open holes.

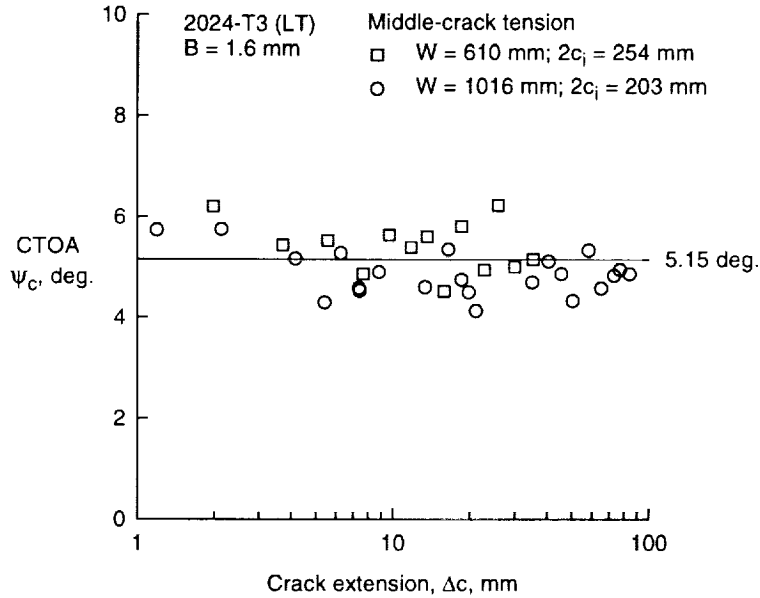


Figure 3. Measured critical CTOA for thin aluminum alloy sheet material.

### 3.1 STAGS FINITE-ELEMENT ANALYSES

STAGS is a finite element program for the analysis of general shell-type structures [14,15]. The program has several types of analysis capabilities (static, dynamic, buckling, crack extension, material nonlinear and geometric nonlinear behavior). STAGS has crack extension capability based on the critical crack-tip-opening angle or displacement (CTOA or CTOD) criterion, the T\*-integral [17] and the traditional  $K_R$ -curve. In the current study, quadrilateral shell elements with 6 degrees-of-freedom per node (three displacements and three rotations) were used in all model. The quadrilateral shell element was under “plane-stress” conditions everywhere in the model except for a “core” of elements along the crack plane that were under “plane strain” conditions [16]. Elastic-plastic material behavior of the sheet and stiffener were approximated by multi-linear stress-strain curves. The White-Besseling plasticity theory with a form of kinematic hardening was used to account for yielding and reverse yielding during unloading [14].

In this section, the procedures used in modeling the stiffened panels and the crucial issues related to rivet flexibility are discussed. Before analyzing these wide stiffened panels, a preliminary study (both experimental and numerical) was carried out to understand the basic concepts of load transfer in built-up structure using a laboratory coupon specimen. For this purpose, 305-mm wide center-cracked panels with a single central stiffener was tested and analyzed. Both cut and intact stiffener situations were considered. The specimens were strain-gaged to measure sheet and stiffener strains (and load transfer) as a function of remote load and crack extension. This particular study helped in understanding the important issues involved in modeling rivet flexibility and sheet-stiffener contact during buckling of the specimen. Comparison between the experiments and the analysis were made at both global and local levels. Load transfer through the rivets near to the crack-tip region were compared with test results. Further details on these tests are given in references 7 and 8.

The specimen configuration and a typical finite-element model for the stiffened panel are shown in Figures 1(a) and 4, respectively. Because the configuration and loading were symmetric, only a quarter of the sheet and stiffeners was modeled. Figure 4 shows only the lower part of the mesh pattern used to model the lead crack and MSD. The mesh pattern to model the upper part of the specimen (not shown) is

similar to that shown in the upper part of Figure 4. The remote loading was applied as uniform displacement. Symmetry boundary conditions were applied along the specimen centerlines except for the crack surfaces that were free. This model contained 13,145 shell elements, 17,287 nodes, 97,254 degree-of-freedom (DOF) and 82,372 active DOF.

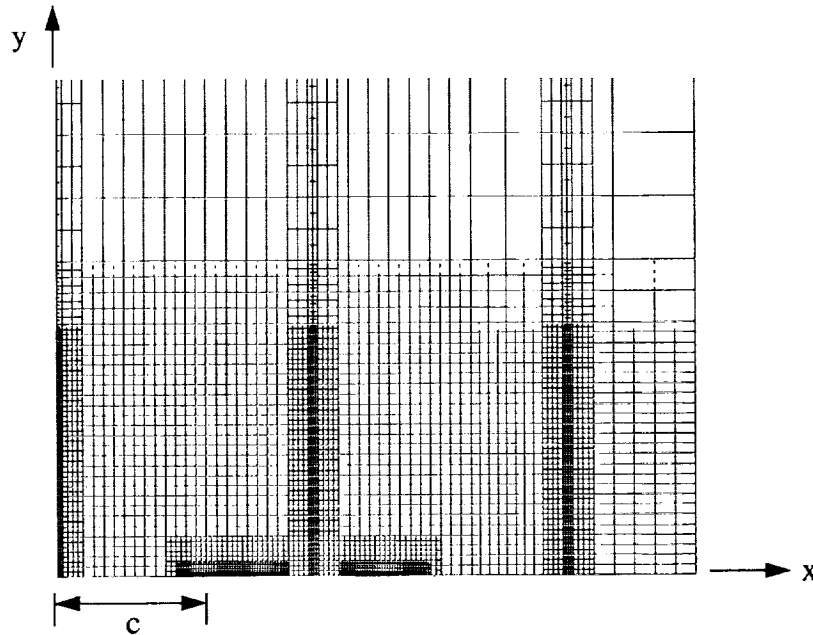


Figure 4. Typical finite-element model of flat, stiffened panel with single and MSD cracks.

### 3.1.1 Modeling of Sheet and MSD Cracking

To model the fracture process with the CTOA failure criterion, a model with an array of small elements were positioned along the crack plane. A minimum crack-tip element size ( $d$ ) of 1 mm, along the line of crack extension, was chosen to be the same for all meshes generated for the different crack configurations. From previous parametric and convergence studies, it was found that a minimum crack-tip element size of 1 mm (linear-strain element) was sufficient to model stable tearing under elastic-plastic conditions [18]. Crack growth was governed by monitoring the critical CTOA ( $\psi_c$ ) at a distance of 1 mm (one element) behind the crack tip. In general, the critical value ( $\psi_c$ ) was determined by matching the average failure load measured on several tests of M(T) specimens (restrained from buckling), as will be discussed later.

The MSD crack sizes in the tests were 0.0 (no crack), 0.25, 0.76 and 1.3-mm in length from the open holes, see Figure 1(b). Because the MSD crack sizes were smaller than the 1-mm crack-tip element size, the circular holes were not modeled. To model MSD cracks, the displacement conditions for the nodes along the symmetric plane over the diameter of the hole and MSD cracks were set free. The total crack lengths for the four MSD cases were: 4.8 (hole diameter), 5.3, 6.3 and 7.4-mm, respectively. In the analyses, the corresponding crack lengths were set at: 5, 5, 6 and 7-mm, respectively. For the single crack and open hole only configurations, the “crack” which was used to simulate the unsupported hole region had a critical CTOA (24 degs.) large enough to prevent crack growth. Whereas, the lead crack had a constant tearing CTOA from initiation to failure. Crack linkup occurred under constant CTOA conditions for all crack tips. An option to have a crack-initiation displacement,  $\delta_i$ , or CTOA,  $\psi_i$ ,

different than the tearing CTOA,  $\psi_c$ , has recently been added to the STAGS code [15]. This option is used to simulate fracture of “sawcuts” and stable tearing of cracks [19]. This option was not used in the current study to simulate fracture of open holes connected by a crack (sharp-notch configuration). Only stable tearing until the crack linked up with the first open hole was considered.

### 3.1.2 Modeling of Stiffeners and Rivets

Analyses of cracked-stiffened panels by Newman and Dawicke [11] indicated that a refined mesh was required in the region of the rivet connection to maintain proper load transfer. In the 1016-mm wide stiffened panels, the elements in the rivet-connection region were 2 mm by 2 mm. Larger elements were used away from the rivet connection and away from the crack plane to help reduce the number of degrees-of-freedom. The stiffeners were modeled separately and overlapped the sheet with an offset equal to the sheet thickness. Rivet holes were not modeled.

Rivet connections between the stiffener and sheet were modeled with fastener elements in STAGS. The fastener elements are non-linear spring elements with six degrees-of-freedom (three translations and three rotations). For each degree-of-freedom, the user has to input the non-linear load-displacement curve. Rigid links were used at the end of each fastener to distribute the load transferred across each rivet. Rivet holes were again not modeled (a tight fit between the rivet and hole was assumed). For more information on the fastener element capability in STAGS, refer to references 14 and 15.

### 3.1.3 Modeling Buckling and Stiffener-Sheet Contact

Seshadri and Newman [13] have demonstrated that stable tearing in the presence of buckling can be predicted with STAGS and the CTOA fracture criterion. In order to simulate buckling of both the stiffened and unstiffened panels, a bifurcation analysis was conducted to determine the first buckling mode shape. This out-of-plane displacement shape (about 10% of the sheet thickness) was then introduced as an imperfection in the sheet for the non-linear analysis. The sheet and stiffener surfaces penetrated each other as they deformed out-of-plane. To prevent penetration, contact elements and multi-point constraint conditions were used to allow the sheet and stiffener surfaces to contact or separate during buckling.

### 3.1.4 Modeling of Crack-Tip Constraint

A concept of defining plane-strain elements around the crack-front region was adopted to simulate three-dimensional constraint conditions around a crack front [16]. Previous analyses of wide flat panels [12] have shown that the high constraint conditions around a crack front, like plane strain, has to be modeled in order for the critical CTOA criterion to predict wide panel failure from small laboratory tests. The plane-strain core capability has recently been added to the STAGS code [15]. The plane-strain core is defined as a strip of elements ( $h_c$  is half-height) parallel to the crack plane. In the present analyses, the core height was selected as 2 mm to help fit the failure loads on various width M(T) specimens.

## 3.2 DETERMINATION OF THE CRITICAL CTOA

A critical CTOA ( $\psi_c$ ) value was used to model the onset of crack growth and the stable tearing process. This criterion is equivalent to a critical CTOD ( $\delta_c$ ) value at a specified distance behind the crack tip. At each load increment, the CTOA was calculated and compared to a critical value  $\psi_c$ . When the CTOA exceeded the critical value, the crack-tip node was released and the crack was advanced to the next node. This process was continued until crack growth became unstable under load control or until the desired

crack length had been reached under displacement control. For multiple-site-damage cracking analyses, all cracks were controlled by the same critical CTOA at each crack tip. The load-crack-extension results on the single crack in the 1016-mm wide panel was used to determine the critical CTOA ( $\psi_c$ ) by trial-and-error. Figure 5(a) shows the measured load-against-crack extension results (symbols) from only one-side ( $x > 0$ ) of the wide panel. The use of the digital-image correlation system to measure out-of-plane displacements prevented crack-extension measurements from the other side ( $x < 0$ ) of the panel, thus crack extension was assumed to be symmetric. A value of  $\psi_c = 5.4$  degrees was found to fit the maximum load quite well. The calculated results from the analysis tended to over predict crack extension after crack initiation. This behavior has been a general trend that has been observed on many other tests and analyses [10-13]. At first glance, a higher CTOA at initiation than during stable tearing would fit the test data better. However, the plastic history generated during fatigue pre-cracking was not modeled because this capability has not been incorporated into STAGS. It was estimated that fatigue pre-cracking would raise the initial portion of the predicted curve by about 10 kN. Also, a crack in the thin-sheet material severely tunnels at crack initiation, as much as two times the sheet thickness, so the surface measurement of crack extension is low compared to the interior [12]. These two issues would tend to make the predicted results with a constant CTOA in better agreement with the test data. A comparison of the measured and calculated load-against-crack-opening displacements at the center of the crack are shown in Figure 5(b). Here the calculated results agreed well with the test measurements.

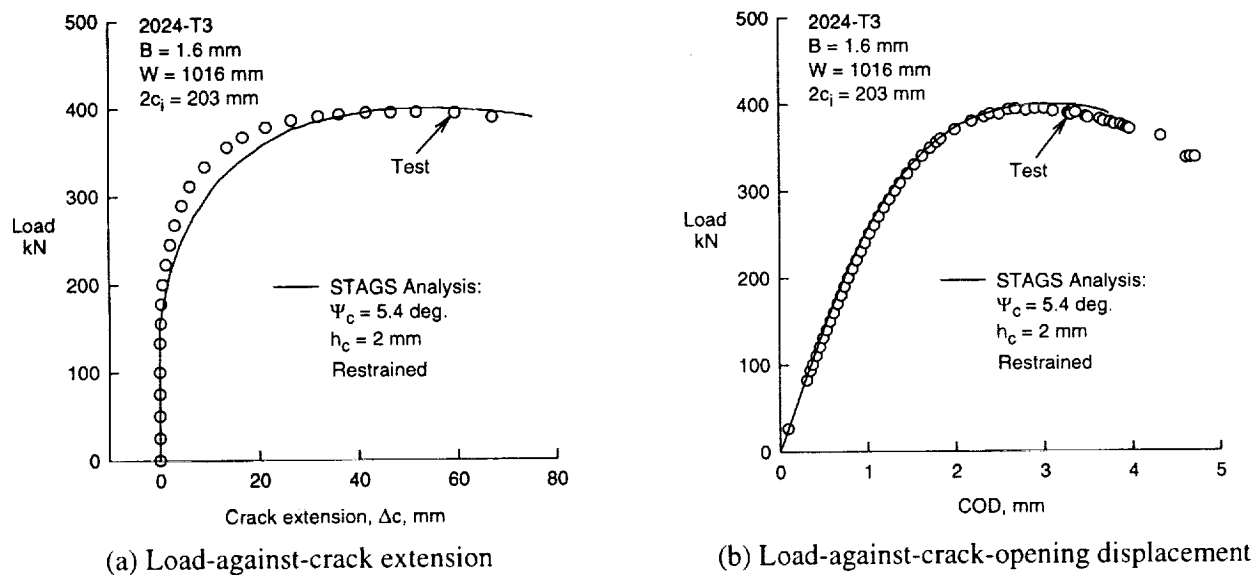


Figure 5. Measured and calculated load-against-crack extension and displacements using CTOA.

The value of CTOA (5.4 deg.) needed to fit the wide panel test results using the finite-element analyses was slightly larger than the average value (5.15 deg.) measured on the same wide panel (Fig. 3). There could be numerous reasons why these values do not agree. First, the measurements are made on the surface of the specimen and fracture is controlled by the deformation state in the interior. To minimize the number of degrees-of-freedom in structural analyses, the crack-tip element size has been selected to be about 1-mm in size. Smaller element sizes will support larger strains and leave larger residual plastic deformations and, possibly, smaller CTOA values. The finite-element analyses assume small strain

and crack-tip deformations occur under large-strain conditions. However, measurements and analyses tend to indicate that the critical CTOA is nearly constant for large amounts of stable tearing and for conditions of extreme plastic deformations.

Fracture tests conducted on smaller middle-crack tension M(T) and compact tension C(T) specimens were analyzed with the STAGS code and the critical CTOA of 5.4 degrees with the same plane-strain core size. Predicted failure loads on tests conducted on 305 and 610-mm wide M(T) specimens, restrained and un-restrained from buckling, were within  $\pm 5\%$  of the test failure loads, but the predicted failure load on a 152-mm wide C(T) specimen was 8% lower than the average test failure load from several tests.

### 3.3 FRACTURE ANALYSIS OF UNSTIFFENED PANELS

STAGS and the critical CTOA determined from restrained wide panel tests were used to predict stable crack growth behavior of wide unstiffened panels with a single crack, a single crack with multiple open holes, and a single crack with MSD at each open hole. These panels were allowed to buckle. These predictions (curves) are compared with the test results (symbols) in Figure 6. The predicted results for a single crack agreed well with test data up to about 15 mm of crack extension. Here the test data reached a plateau and failed after a crack extension of about 35 mm. The predicted failure load was about 10% higher than the test load. For the single crack and open holes, the predicted stable tearing behavior as the

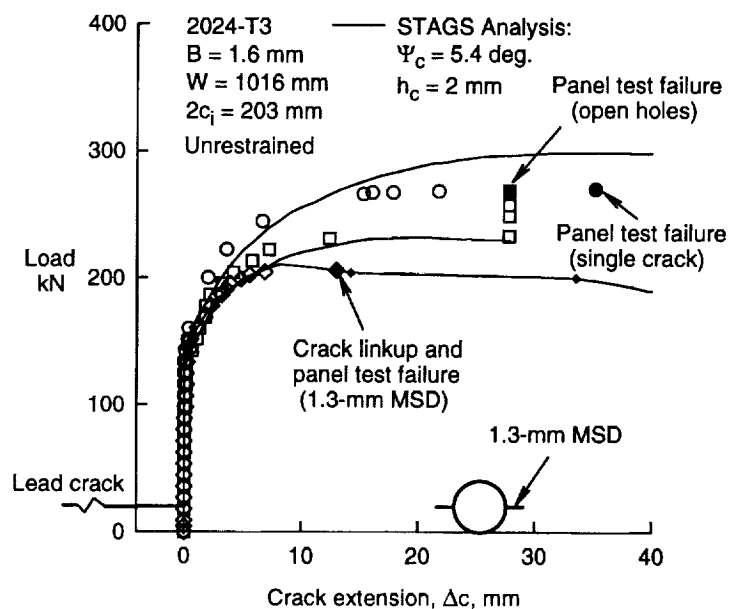


Figure 6. Measured and predicted load-against-crack extension for unstiffened panels.

crack linked up with the first open hole agreed well with test measurements. The insert shows the lead crack and location of the first hole. The panel failed at a load (15%) higher than the crack-hole linkup load, but no attempt was made to model the fracture of a sharp-notch configuration (crack connecting two holes). For the single crack with the 1.3-mm MSD, the lead crack and the MSD crack both grew and linked up when the lead crack had grown about 13 mm. The panel failed at the first linkup of the lead crack and the MSD crack (large solid diamond symbol). The small solid symbols show the calculated MSD crack size at linkup. The predicted maximum load, at about 8 mm of crack extension, agreed well with the test failure load. The remaining curve is the predicted behavior under displacement control.

### 3.4 FRACTURE ANALYSIS OF STIFFENED PANELS

The stable crack growth behavior of wide stiffened panels with a single crack and a single crack with MSD at each open hole was predicted using STAGS and the critical CTOA value. Again, these panels were allowed to buckle. Figure 7 shows the test measurements (symbols) made on the panel with a single crack. The insert shows the relative location of the stiffener. Crack extension was measured until the crack went underneath the stiffener. Once the crack grew outside of the stiffener, the panel failed (solid symbols). Whether failure of the panel was due to sheet failure or stiffener failure could not be determined. Failure of either would immediately result in panel failure because the stiffeners were carrying about one-half of the applied load.

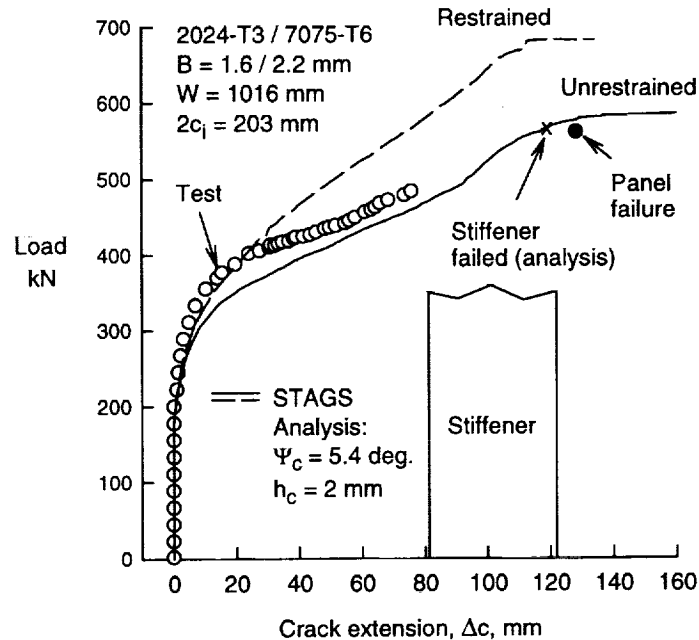


Figure 7. Measured and predicted load-against-crack extension for stiffened panel with single crack.

Two predictions were made using STAGS. First, the panel was restrained against buckling and the predicted results are shown by the dashed curve in Figure 7. After 20 mm of crack extension the restrained analysis tended to significantly over predict the test data and the predicted failure load was much higher than the test failure load. However, the unrestrained analysis (buckling allowed) under predicted the early stages of stable tearing but agreed well after about 30 mm of crack extension, similar to the results shown in Figure 5(a). The predicted failure load from the fracture of the sheet was 4% higher than the test failure load. The calculated stiffener failure load (x symbol) was extremely close to the actual test failure load. (Stiffener failure load was based on fracture tests conducted on the 305-mm wide specimens with a single intact stiffener at  $x = 0$  [7,8].)

A comparison of the measured and predicted load-against-crack extension for the wide stiffened panel with a lead crack and the 1.3-mm MSD is shown in Figure 8. The insert shows the relative location of the lead crack, open holes, MSD, and the intact stiffener. The measured load-crack extension values for the data underneath the stiffener were inferred from the load-time trace recorded on this specimen. As the crack linked up with the open hole at about 125 mm, the sheet failed with all 24 MSD cracks linking. Panel failure then occurred at about a 10% higher load to break the stiffeners. The predicted load-crack extension behavior matched the test results very well. These results indicated that the STAGS code and

the CTOA failure criterion could predict stable tearing in the presence of MSD in a stiffened structure with severe out-of-plane deformations, typical of what may occur in an aircraft fuselage under pressure.

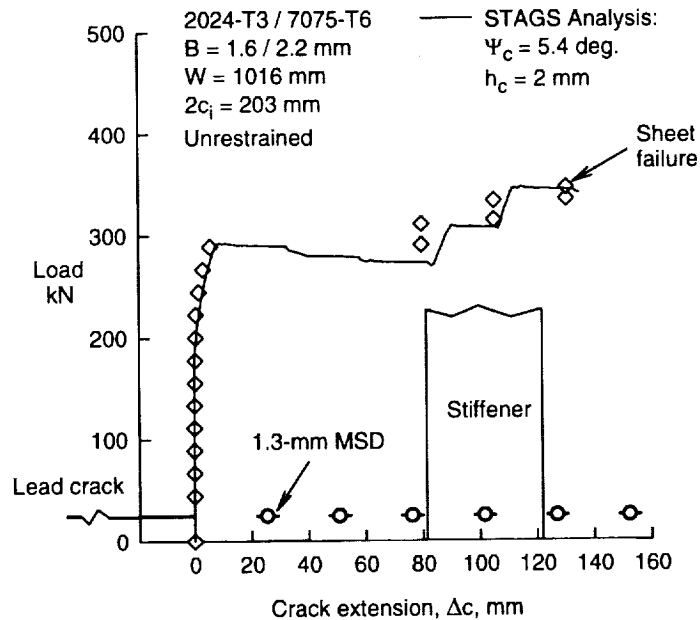


Figure 8. Measured and predicted load-crack extension for stiffened panel with crack and 1.3-mm MSD.

#### 4. CONCLUSIONS

The STAGS finite-element code and the CTOA fracture criterion were used to predict stable tearing and residual strength of 1016-mm wide stiffened panels made of 2024-T3 aluminum alloy sheet with 7075-T6 stiffeners. The panels had a single crack, a single crack with 12 open holes, and a single crack with 12 equal-size and equally-spaced multiple-site damage (MSD) cracks. A similar series of tests were also conducted on unstiffened panels. This work supports the following conclusions:

- (1) The measured critical crack-tip-opening angle (CTOA) was nearly constant over two orders of magnitude of crack extension for the thin-sheet 2024-T3 aluminum alloy.
- (2) A constant critical crack-tip-opening angle (CTOA),  $\Psi_c = 5.4$  degrees, with the plane-strain core and STAGS were able to predict stable tearing behavior and residual strength of 152 to 1016-mm wide specimens within  $\pm 10\%$ .
- (3) A constant critical crack-tip-opening angle (CTOA),  $\Psi_c = 5.4$  degrees, with the plane-strain core and STAGS were able to predict stable tearing behavior and residual strength of wide stiffened panels with single cracks and MSD under severe buckling within 5%.

#### 5. ACKNOWLEDGMENTS

The authors wish to thank Mr. Tom Swift, FAA Retired, for guidance in designing the stiffened panels and Dr. Charles Rankin, Lockheed Palo Alto Research Laboratory, for incorporating the plane-strain core and the CTOA options into the STAGS code.

## 6. REFERENCES

- [1] Swift, T., "Damage Tolerance in Pressurized Fuselages", New Materials and Fatigue Resistant Aircraft Design, D. L. Simpson, ed., EMAS Ltd., 1987, pp. 1-77.
- [2] Maclin, J., "Performance of Fuselage Pressure Structure," International Conference on Aging Aircraft and Structural Airworthiness, C. E. Harris, ed., NASA CP-3160, Washington, D.C., 1992, pp. 67-75.
- [3] McGuire, J. F. and Goranson, U. G., "Structural Integrity of Future Aging Airplanes", 1991 International Conference on Aging Aircraft and Structural Airworthiness, C. E. Harris, ed., NASA CP-3160, Washington, D.C., 1992, pp. 33-48.
- [4] Harris, C. E.; Newman, J. C., Jr.; Piascik, R. and Starnes, J. H., Jr., "Analytical Methodology for Predicting the Onset of Widespread Fatigue Damage in Fuselage Structure", *Journal of Aircraft*, Vol. 35, No. 2, 1998, pp. 307-317.
- [5] Dawicke, D. S.; Gullerud, A. S.; Dodds, R. H. and Hampton, R., "Residual Strength Predictions with Crack Bulging," 2nd Joint NASA/FAA/DoD Conference on Aging Aircraft, Williamsburg, VA, 1998.
- [6] Young, R. D.; Rouse, M.; Ambur, D. R. and Starnes, J. H., Jr., "Residual Strength Pressure Tests and Nonlinear Analyses of Stringer- and Frame-Stiffened Aluminum Fuselage Panels with Longitudinal Cracks," Second Joint NASA/FAA/DoD Conference on Aging Aircraft, Williamsburg, VA., 1998.
- [7] Dawicke, D. S.; Newman, J. C., Jr. and Tan, P. W., "FAA/NASA Wide Panel Fracture Tests - Part I Executive Summary," NASA TM (in progress), 1998.
- [8] Johnston, W. M. and Helm, J. D., "FAA/NASA Wide Panel Fracture Tests - Part II Experimental Test Program," NASA CR (in progress), 1998.
- [9] Kanninen, M.; Rybicki, E.; Stonesifer, R.; Broek, D.; Rosenfield, A. and Nalin, G., "Elastic-Plastic Fracture Mechanics for Two-Dimensional Stable Crack Growth and Instability Problems", ASTM STP 668, 1979, pp. 121-150.
- [10] Dawicke, D. S.; Sutton, M. A.; Newman, J. C., Jr. and Bigelow, C. A., "Measurement and Analysis of Critical CTOA for Thin-Sheet Aluminum Alloy Materials", Fracture Mechanics: 25th Volume, ASTM STP 1220, F. Erdogan, ed., 1995, pp. 358-379.
- [11] Newman, J. C., Jr. and Dawicke, D. S., "Fracture Analysis of Stiffened Panels under Biaxial Loading with Widespread Cracking," AGARD CP-568, 1995, pp. 3.1-3.16.
- [12] Dawicke, D. S.; Newman, J. C., Jr. and Bigelow, C. A., "Three-Dimensional CTOA and Constraint Effects during Stable Tearing in a Thin-Sheet Material," Fracture Mechanics: 26th Volume, ASTM STP 1256, W. G. Reuter, J. H. Underwood and J. C. Newman, Jr., eds., 1995, pp. 223-242.
- [13] Seshadri, B. R. and Newman, J. C., Jr., "Analyses of Buckling and Stable Tearing in Thin-Sheet Materials," Fatigue and Fracture Mechanics: 29th Volume, ASTM STP 1332, T. L. Panontin and S. D. Sheppard, eds., 1998.
- [14] Almroth, B.; Brogan, F. and Stanley, G., "User's Manual for STAGS", NASA CR 165670, 1978.
- [15] Rankin, C. C.; Brogan, F. A.; Loden, W. A. and Cabiness, H. D., "STAGS User Manual - Version 2.4," Lockheed Martin Advanced Technology Center, Report LMSC P032594, 1997.
- [16] Newman, J. C., Jr.; Booth, B. C. and Shivakumar, K. N., "An Elastic-Plastic Finite-Element Analysis of the J-Resistance Curve using a CTOD Criterion", Fracture Mechanics: 18th Volume, ASTM STP 945, D. T. Read and R. P. Reed, eds., 1988, pp. 665-685.
- [17] Atluri, S. N. and Tong, P., "Computational Schemes for Integrity Analyses of Fuselage Panels in Aging Airplanes," *Structural Integrity of Aging Airplanes*, Springer-Verlag, 1991, pp. 33.
- [18] Dawicke, D. S. and Newman, J. C., Jr., "Residual Strength Predictions for Multiple-Site Damage Cracking using a CTOA Criterion," Fatigue and Fracture Mechanics: 29th Volume, ASTM STP 1332, T. L. Panontin and S. D. Sheppard, eds., 1998.
- [19] Newman, J. C., Jr., Dawicke, D. S., Sutton, M. A. and Bigelow, C. A., "A Fracture Criterion for Widespread Cracking in Thin-Sheet Aluminum Alloys," Durability and Structural Integrity of Airplanes, Vol. I, A. F. Blom, ed., EMAS Ltd., 1993, pp. 443-468.